



## The effect of mAb and excipient cryoconcentration on long-term frozen storage stability – part 2: Aggregate formation and oxidation

Oliver Bluemel<sup>a</sup>, Jakob W. Buecheler<sup>b</sup>, Astrid Hauptmann<sup>c</sup>, Georg Hoelzl<sup>c</sup>, Karoline Bechtold-Peters<sup>b</sup>, Wolfgang Friess<sup>a,\*</sup>

<sup>a</sup> Pharmaceutical Technology and Biopharmaceutics, Department of Pharmacy, Ludwig-Maximilians-Universitaet Muenchen, 81377 Munich, Germany

<sup>b</sup> Technical Research and Development, Novartis Pharma AG, 4002 Basel, Switzerland

<sup>c</sup> Sandoz GmbH, 6336 Langkampfen, Austria

### ARTICLE INFO

#### Keywords:

cryoconcentration  
frozen storage  
large-scale freezing  
monoclonal antibody  
stability

### ABSTRACT

We examined the impact of monoclonal antibody (mAb) and buffer concentration, mimicking the cryoconcentration found upon freezing in a 2 L bottle, on mAb stability during frozen storage. Upon cryoconcentration, larger protein molecules and small excipient molecules freeze-concentrate differently, resulting in different protein to stabiliser ratios within a container. Understanding the impact of these shifted ratios on protein stability is essential. For two mAbs a set of samples with constant mAb (5 mg/mL) or buffer concentration (medium histidine/adipic acid) was prepared and stored for 6 months at  $-10^{\circ}\text{C}$ . Stability was evaluated via size-exclusion chromatography, flow imaging microscopy, UV/Vis spectroscopy at 350 nm, and protein A chromatography. Dynamic light scattering was used to determine  $k_D$  values. Soluble aggregate levels were unaffected by mAb concentration, but increased with histidine concentration. No trend in optical density could be identified. In contrast, increasing mAb or buffer concentration facilitated the formation of subvisible particles. A trend towards attractive protein-protein interactions was seen with higher ionic strength. MAb oxidation levels were negatively affected by increasing histidine concentration, but became less with higher mAb concentration. Small changes in mAb and buffer composition had a significant impact on stability during six-month frozen storage. Thus, preventing cryoconcentration effects in larger freezing containers may improve long-term stability.

### 1. Introduction

Therapeutic proteins, especially monoclonal antibodies (mAbs), are high-value biotechnological products and gained importance in the treatment of a variety of diseases (Arsiccio and Pisano, 2020; Gervasi et al., 2018; Maity et al., 2009; Miller et al., 2013). Numerous technical challenges have to be considered during production, storage, and transportation (Hauptmann et al., 2019). Freezing of bulk protein solution is commonly used to increase chemical and physical stability (Padala et al., 2010). By decoupling drug substance and drug product processing, frozen storage and transportation offers manufacturing flexibility (Kolhe et al., 2009; Rodrigues et al., 2011). Additionally, freezing eliminates the risk of shaking and foaming and minimises microbial growth (Padala et al., 2010; Rodrigues et al., 2011). While

controlled freezing and thawing are intentionally performed during production, mishandling may lead to unintentional uncontrolled freezing of drug product. Although freezing is associated with numerous advantages, it also comes with several drawbacks. Detrimental effects from cold denaturation (Arsiccio et al., 2020), denaturation at the ice-liquid interface (Arsiccio and Pisano, 2020; Duarte et al., 2020), crystallisation of excipients and buffers (Connolly et al., 2015; Singh et al., 2011), potentially coming with marked pH shifts (Kolhe et al., 2009; Pikal-Cleland et al., 2000), and especially cryoconcentration (Hauptmann et al., 2019; Kolhe et al., 2012; Roessler et al., 2015) are well described. Growing ice only partially includes solutes (Miller et al., 2013). Most of the solutes are excluded by growing ice crystals and consequently form a freeze-concentrated matrix (FCM), which composition is described by phase or state diagrams (Authelin et al., 2020;

**Abbreviations:** DLS, Dynamic light scattering; FCM, Freeze-concentrated matrix; HMWS, Higher molecular weight species; HPLC, High performance liquid chromatography; HPW, Highly purified water; mAb, Monoclonal antibody; OD350, Optical density at 350 nm; PES, Polyethersulfone; SEC, Size-exclusion chromatography; SVP, Subvisible particle;  $T_g'$ , Glass transition temperature of the maximally freeze-concentrated solution.

\* Corresponding author.

E-mail address: [Wolfgang.Friess@cup.uni-muenchen.de](mailto:Wolfgang.Friess@cup.uni-muenchen.de) (W. Friess).

<https://doi.org/10.1016/j.ijpx.2021.100109>

Received 21 December 2021; Accepted 22 December 2021

Available online 25 December 2021

2590-1567/© 2021 Published by Elsevier B.V. This is an open access article under the CC BY-NC-ND license (<http://creativecommons.org/licenses/by-nc-nd/4.0/>).

Miller et al., 2013). The glass transition temperature of the maximally freeze-concentrated solution ( $T_g'$ ) determines the vitrification of this FCM. In practical terms not only this microscopic cryoconcentration is of interest, but also macroscopic freeze-concentration plays an important role. During freezing, natural convection and diffusion transport proteins and excipients away from the freezing front (Miller et al., 2013). Recent studies outline differences in cryoconcentration of large proteins and small excipients, mainly attributed to differences in diffusivity (Bluemel et al., 2020; Kolhe et al., 2012; Miller et al., 2013). Consequently, a spatial heterogeneity builds up that is mainly driven by the processing conditions. Beside colloidal and conformation instability, the importance of protein oxidation has recently been highlighted (Authelin et al., 2020). Often small-scale studies in tubes, vials or vessels are used to optimise processing conditions, formulation composition, unveil aggregation mechanisms, and examine long-term storage stability (Connolly et al., 2015; Hauptmann et al., 2018; Kuelzto et al., 2008; Miller et al., 2013; Zhang et al., 2012). Miller et al. examined the frozen-state storage stability of a mAb in 50 mL stainless steel cylindrical vessels (Miller et al., 2013). They found that changes in concentration persist over time, regardless of the storage temperature. Furthermore, long-term storage stability is mainly impacted by the solution's  $T_g'$ . Storage below  $T_g'$  completely inhibits aggregation, whereas storage above  $T_g'$  may result in marked aggregation.

Previously, we highlighted significant changes in concentration upon large-scale freezing of mAb solutions and different ratios of mAb to histidine buffer in larger containers due to differences in diffusivity (Bluemel et al., 2020). Miller et al. connected cryoconcentration and long-term stability of frozen mAb solutions (Miller et al., 2013). However, they focused on the freezing conditions rather than the impact of freeze-concentration and shifted protein to excipient ratio.

In the current study, we examine the influence of changes in mAb and buffer concentration on higher molecular weight species (HMWS) levels, subvisible particles (SVPs), optical density at 350 nm (OD350) as well as mAb oxidation. MAb to buffer concentrations and ratios were adjusted in the similar range that evolves during large-scale freezing (Bluemel et al., 2020). All samples were frozen identically to minimise the effect of processing conditions and stored for 6 months at  $-10^\circ\text{C}$ . A temperature above  $T_g'$  was selected to generate a stress model. Thereby, we directly connect cryoconcentration and long-term storage stability. For two human IgG1 mAbs two sets of samples were prepared; one set with fixed mAb concentration (5 mg/mL) and varying buffer concentration (zero to maximum histidine/adipic acid) and a second set that covered variations in mAb concentration (0 mg/mL to 10 mg/mL) at a given buffer concentration (medium histidine/adipic acid).

Increasing mAb concentration did not alter HMWS levels after six-month storage, but led to a higher SVP count. Higher buffer concentrations weakened repulsive protein-protein interactions and decreased mAb storage stability. Both mAbs formulated in highly purified water (HPW) showed highest levels of soluble aggregates, but lowest levels of SVPs. Higher levels of partially oxidised mAb fractions were detected in samples with lower mAb concentration. Oxidation of proteins is most likely induced at the surface of air bubbles that form during freezing (Authelin et al., 2020). In addition, histidine facilitated mAb1 oxidation.

Our study reveals that the little changes in mAb and buffer concentration at the different positions in a large container with frozen drug substance can affect long-term storage stability. Therefore, cryoconcentration should be avoided and the initial formulation composition optimised. In addition to the formation of soluble and insoluble aggregates, mAb oxidation is an important parameter during frozen storage, which should receive more attention in future stability studies.

## 2. Materials and methods

### 2.1. Materials

Novartis AG (Basel, Switzerland) provided IgG1 mAb1 in medium

histidine buffer at pH 5.5 and IgG1 mAb2 in medium adipic acid at pH 5.2 stock solutions. L-histidine monochloride and L-histidine monohydrate were both purchased from Merck KGaA (Darmstadt, Germany). Adipic acid 99% was obtained from Sigma-Aldrich Produktions GmbH (Steinheim am Albuch, Germany).

Dipotassium phosphate, monopotassium phosphate, and disodium phosphate dihydrate were acquired from Merck KGaA (Darmstadt, Germany). Acetic acid and potassium chloride were purchased from VWR International GmbH (Darmstadt, Germany), sodium chloride from Bernd Kraft GmbH (Duisburg, Germany).

Uncoated 2R glass vials from SCHOTT AG (Mainz, Germany) were used. West Pharmaceuticals (Eschweiler, Germany) provided FluroTec® lyophilisation stoppers. Sucrose was obtained from Sigma-Aldrich Produktions GmbH (Steinheim am Albuch, Germany).

Colourless 1.5 mL Eppendorf Tubes® 3810× (Eppendorf AG, Hamburg, Germany) were used for centrifugation.

0.2 µm Polyethersulfone (PES) membrane syringe filters were purchased from VWR International GmbH (Darmstadt, Germany).

Either Slide-A-Lyzer® 12 mL - 30 mL dialysis cassettes (Thermo Fisher Scientific Inc., Waltham, Massachusetts, USA) or Vivaspin® 6 centrifugal concentrators (Sartorius AG, Göttingen, Germany) with a 10 K MWCO were used for dialysis.

### 2.2. Sample preparation

Samples were adjusted as given in Table 1. For the set of samples with constant buffer concentration, mAb1 and mAb2 stock solutions were diluted with a medium histidine buffer pH 5.5 and a medium adipic acid buffer pH 5.2, respectively. Samples with varying buffer concentrations but constant mAb concentration were prepared by diluting stock solutions with differently concentrated buffer solutions. The contribution of the stock solution to the final buffer concentration was considered. For samples with zero buffer, 30 mL of each stock solution was dialysed against HPW using Slide-A-Lyzer® dialysis cassettes. 6 L HPW for each dialysis step were needed to assure complete buffer exchange. Subsequently, these solutions were diluted to 5 mg/mL mAb with HPW. The pH of these samples was measured but not adjusted. The final mAb concentration of all samples was controlled via UV absorption at 280 nm using a NanoDrop™ One (Thermo Fisher Scientific Inc., Waltham, Massachusetts, USA) prior to filtration through 0.2 µm PES syringe filters. For each formulation six 2R glass vials were filled with 1 mL aliquots and semi-stoppered with FluroTec® lyophilisation stoppers. Samples were arranged in the centre of a lyophilisation tray and surrounded by two rows of vials filled with 1 mL of a 10% (w/V) sucrose solution. Subsequently, all vials were frozen in a Christ Epsilon 2-6D LSCplus (Martin Christ Gefrierungsanlagen GmbH, Osterode am Harz, Germany). Samples were cooled to  $-5^\circ\text{C}$  with a rate of 1 K/min. During a 60 min plateau at  $-5^\circ\text{C}$  the ice fog technology induced controlled nucleation. After nucleation a 1 K/min ramp was applied to  $-40^\circ\text{C}$ . Immediately after the freezing run all samples were transferred to a precooled  $-10^\circ\text{C}$  tritec® TC 231 freezer (tritec® Gesellschaft für Labortechnik und Umweltsimulation mbH, Hannover, Germany). To compensate any temperature fluctuations in the freezer, samples were placed inside a polystyrene thermobox. The t0 samples were kept for 12 h at  $-10^\circ\text{C}$ .

### 2.3. Stability analysis

Triplicates were thawed at room temperature on the laboratory bench prior to characterisation.

#### 2.3.1. Flow imaging microscopy

SVPs were analysed using a FlowCam® 8100 (Fluid Imaging Technologies, Inc., Scarborough, Maine, USA) equipped with a 10× magnification cell with 160 µL sample volume and a 0.15 mL/min flow rate. Distance to the nearest neighbour for particle identification was 3 µm.

**Table 1**

Samples overview; for both mAbs a set of samples with constant buffer and constant mAb concentration was prepared.

Histidine	mAb1					medium	high	max
	zero	low	medium	high	max			
mAb [mg/mL]	0	2.5	5	7.5	10	5		

Adipic Acid	mAb2					medium	high	max
	zero	low	medium	high	max			
mAb [mg/mL]	0	2.5	5	7.5	10	5		

Particle segmentation thresholds were 10 for light and 13 for dark pixels. The auto image frame rate was set to 28 frames/s and sampling time to 60 s. Particle size was reported as the equivalent spherical diameter. For measurements and analysis, the VisualSpreadsheet® 4.7.6 software was used.

### 2.3.2. Size-exclusion chromatography

An Agilent 1200 high performance liquid chromatography (HPLC) system equipped with a diode array detector (Agilent Technologies, Santa Clara, California, USA) was used to quantify HMWS via size-exclusion chromatography (SEC). A TSKgel G3000 SWxl column (Tosoh Bioscience GmbH, Griesheim, Germany) at 30 °C served as stationary phase, 150 mM potassium phosphate buffer pH 6.5 as mobile phase at a flow rate of 0.4 mL/min. All samples were diluted to 0.75 mg/mL with mobile phase and 100 µL diluted sample were centrifuged 2 min in 1.5 mL tubes at 25700 x g with a Heraeus™ Megafuge™ 16R (Thermo Fisher Scientific Inc., Waltham, Massachusetts, USA). 10 µL of the supernatant were analysed at 210 nm. Chromatograms were evaluated with the Agilent OpenLAB Data Analysis Software version 2.1.

### 2.3.3. Optical density at 350 nm

The OD350 of 200 µL sample was measured using a FLUOstar® Omega microplate reader (BMG LABTECH GmbH, Ortenberg, Germany) in a quartz 96 microwell plate (Hellma Holding GmbH, Müllheim, Germany).

### 2.3.4. Protein A analytical chromatography

mAb oxidation was evaluated via Protein A chromatography with an Agilent 1200 HPLC system (Agilent Technologies, Santa Clara, California, USA) detecting at 280 nm. The method was adapted from Loew et al. (Loew et al., 2012). Briefly, the stationary phase, an Applied Biosystems™ POROS™ A (4.6 mmD × 50 mmL) column (Thermo Fisher Scientific Inc., Waltham, Massachusetts, USA), was kept at 23 °C and 250 µg mAb were injected. Elution was performed at 2.0 mL/min in a gradient mode with buffer A (Dulbecco's phosphate buffered saline 1 × in HPW at pH 7.4) and buffer B (100 mM acetic acid with 150 mM sodium chloride in HPW at pH 2.8) at 0:0, 40:60, 41:100, 51:100, 52:0, 62:0 (time [minutes]:buffer B [percentage]). 200 µL samples were centrifuged with a Heraeus™ Megafuge™ 16R (Thermo Fisher Scientific Inc., Waltham, MA, USA) at 25700 x g in 1.5 mL tubes.

### 2.4. Determination of the interaction parameter $k_D$

mAb1 and mAb2 stock solutions were dialysed against histidine and adipic acid buffers (low – maximum), respectively. Therefore, 1 mL stock solution was diluted 1:5 with the respective buffer and spun in a Vivaspin® 6 at 4000 x g until approximately 1 mL diluted sample was left. This process was repeated three times to assure sufficient buffer exchange. Finally, samples were diluted to concentrations between 1 mg/mL and 8 mg/mL and filtered through 0.2 µm PES syringe filters.

Dynamic light scattering (DLS) measurements were performed on a DynaPro Plate Reader III (Wyatt Technology, Dernbach, Germany) with 25 µL sample in a 384-well plate (Corning Inc., Corning, New York, USA), centrifuged at 2000 rpm for 2 min using the Heraeus™

Megafuge™ 16R (Thermo Fisher Scientific Inc., Waltham, Massachusetts, USA) with an M-20 microplate swinging-bucket rotor (Thermo Fisher Scientific Inc., Waltham, Massachusetts, USA). Each well was sealed with 5 µL silicon oil and the plate was centrifuged again. All samples were analysed in triplicates with 20 acquisitions of 5 s at 25 °C. The Dynamics V7.8.2.18 software was used to analyse recorded auto-correlation functions and to calculate diffusion coefficients. The linear fit of diffusion coefficient versus protein concentration allows to calculate the interaction parameter  $k_D$  (Menzen and Friess, 2014; Pindrus et al., 2018; Sorret et al., 2016).

## 3. Results

The formation of HMWS and SVPs, changes in OD350, and mAb oxidation upon six-month storage at –10 °C were analysed to evaluate the long-term stability of two mAbs in either histidine or adipic acid buffer. Our main objective was to highlight the contribution of mAb as well as buffer concentration on stability during frozen storage. Two sets of samples were prepared for each mAb (Table 1), reflecting the concentration range found upon large-scale freezing of drug substance in 2 L bottles (Bluemel et al., 2020). Additionally, protein-protein interactions in the formulations were assessed via the interaction parameter  $k_D$ .

### 3.1. Formation of HMWS

The formation of HMWS for both set of samples and both mAbs are shown in Fig. 1. The mAb1 samples showed 1.6% HMWS at the start of the experiment except for samples in HPW with 2.0%. It is important to note that also the t0 samples were subject to freezing and thawing. After 6 months storage, samples with varying mAb1 concentration displayed only marginally increased aggregate levels between 1.7% and 1.9%, independent of the mAb concentration. Overall, the aggregate formation indicates a general mobility in the given formulations at –10 °C as expected upon storage above  $T_g'$  (Pansare and Patel, 2016); differential scanning calorimetry showed  $T_g'$  values between –38 °C and –30 °C and between –59 °C and –45 °C for formulations with histidine and adipic acid, respectively. With increasing histidine concentration aggregation levels after 6 months at –10 °C increased from 1.9% (low histidine) to 6.4% (maximum histidine). The highest HMWS level of 7.6% was detected for mAb1 samples without any histidine, which had a slightly higher pH value of 5.9 compared to the histidine samples buffered to pH 5.5.

The mAb2 samples showed 0.2% soluble aggregates at the start of the experiment, except for the buffer-free sample with 0.6% HMWS. After 6 months frozen storage, HMWS levels were only slightly increased to 0.3%, regardless of the mAb or adipic acid concentration. Marked aggregation was detected for the buffer-free formulation with 6.4% HMWS. These samples had a pH of 5.7 compared to the formulations buffered with adipic acid at 5.2.

### 3.2. Formation of subvisible particles

In the medium histidine buffer control less than 1200 SVPs  $\geq 1 \mu\text{m}$  at the start and after 6 months at –10 °C were detected (Fig. 2). At the

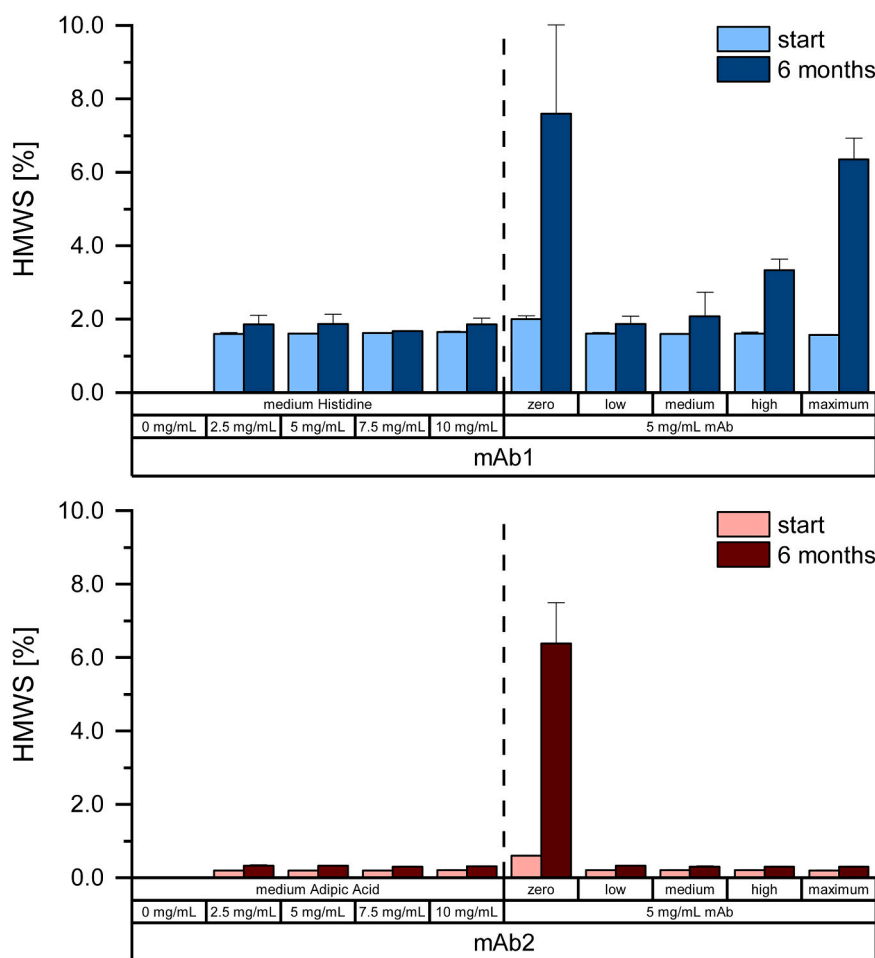


Fig. 1. HMWS levels at the start and after six-month storage at  $-10^{\circ}\text{C}$ .

start, up to 10200 SVPs  $\geq 1\ \mu\text{m}$  were detected in mAb1 samples without a trend with increasing histidine concentration. However, an increase in protein concentration from 2.5 mg/mL to 10 mg/mL mAb1 resulted in an increase in SVPs from 2400 to 8300. After six months storage at  $-10^{\circ}\text{C}$ , clear trends in SVPs were seen. With increasing mAb1 concentration from 2.5 mg/mL to 10 mg/mL the SVP count rose from 40300 to 101300 SVPs. Higher histidine concentrations decreased the colloidal stability. Samples without histidine displayed only 13800 insoluble aggregates, but particle levels steadily increased to 22000 (low histidine), 45200 (medium histidine), 83600 (high histidine), and 166100 (maximum histidine). In both sample sets, samples with 5 mg/mL mAb1 in medium histidine buffer did not differ significantly in respect of SVP count.

The medium adipic acid buffer control sample showed less than 1000 SVPs  $\geq 1\ \mu\text{m}$  at the start and after 6 months. At  $t_0$ , SVPs were low and independent of the adipic acid concentration, but increasing with mAb2 concentration from 2300 to 6300. The negative impact of mAb and buffer concentration on colloidal stability during long-term storage seen for mAb1 in histidine buffer was confirmed by the results for mAb2 in adipic acid buffer. SVP formation was more pronounced at higher mAb concentration increasing from 52300 at 2.5 mg/mL mAb2 to 166700 at 10 mg/mL mAb2. Similarly, the adipic acid concentration had a negative impact with 45800 SVPs at low adipic acid to 95200 at maximum adipic acid concentration. Samples without adipic acid showed 24300 SVPs at the start without further SVP formation upon storage.

### 3.3. Optical density at 350 nm

Aggregate formation affecting turbidity was covered by analysis of OD350. At  $t_0$  the OD350 was between 0.039 and 0.054, increasing slightly with mAb concentration (Fig. 3). There was no clear trend in the change in OD350 after six-month frozen storage and in many samples no change was detectable.

### 3.4. MAb oxidation

Additionally, mAb oxidation was analysed by protein A chromatography. Three peaks for different degrees of methionine oxidation in the Fc part can occur (Loew et al., 2012). We did not observe the peak reflecting full oxidation of Met252 and strongly oxidised Met428, but detected partially oxidised species. Oxidation of mAb1 was between 3.3% and 4.5% at  $t_0$  (Fig. 4). Upon six-month storage, samples with lowest mAb1 concentration showed 7.7% oxidised species. With increasing mAb1 concentration the oxidised fraction became less and at 10 mg/mL mAb1 only 5.0% oxidised species were detected. Mab oxidation increased with higher histidine concentration respectively mAb storage stability slightly decreased, as only 4.9% partially oxidised mAb1 were detected in the histidine free formulation, while 7.4% were observed at maximum histidine.

Initially, mAb2 samples in adipic acid showed between 1.4% and 2.5% oxidation. During frozen storage, the partially oxidised fraction increased but less than for mAb1 in histidine. The mAb concentration again had a positive impact with 3.8% oxidised species at 2.5 mg/mL mAb2 compared to 2.5% at 10 mg/mL. The increase in oxidised species

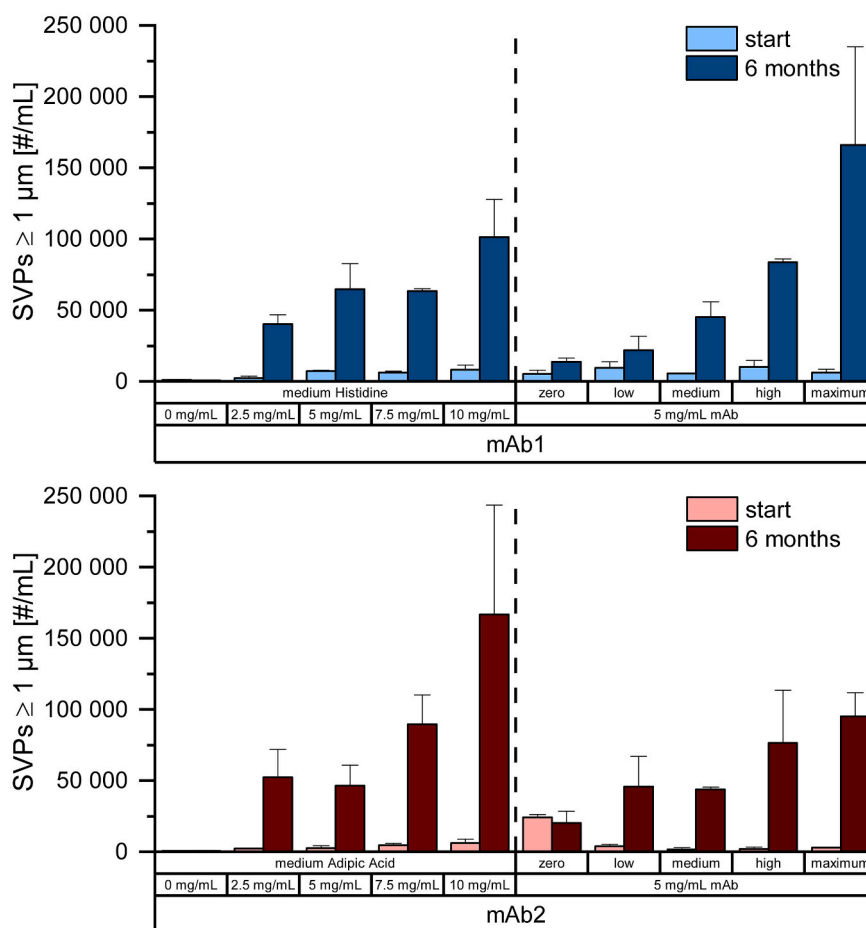


Fig. 2. SVPs  $\geq 1 \mu\text{m}$  at the start and after six-month storage at  $-10 \text{ }^\circ\text{C}$ .

by approximately 1.2% upon storage was independent of the adipic acid concentrations (samples with high adipic acid concentration displayed the highest oxidised fraction after 6 months with 4.4%, but also had the highest level at t0).

### 3.5. Interaction parameter $k_D$

The linear fit of mutual diffusion coefficients versus mAb concentration allows to calculate the interaction parameter  $k_D$  (Menzen and Friess, 2014; Pindrus et al., 2018; Sorret et al., 2016). While it was possible to evaluate the effect of histidine and adipic acid on mAb self-interaction,  $k_D$  analysis at low ionic strength has to be carefully interpreted because of nonlinearity of the experimental data (Pindrus et al., 2018; Sorret et al., 2016). We therefore excluded buffer-free formulations. Increasing histidine concentration reduced mAb1  $k_D$  values from 24.6 mL/g to 1.8 mL/g (Fig. 5). The  $k_D$  value of mAb2 decreased from 3.0 mL/g in low adipic acid to a negative value of  $-4.2 \text{ mL/g}$  in maximum adipic acid.

## 4. Discussion

Our aim was to close the knowledge gap about the stability of frozen bulk drug substance, which is regularly utilised in production of protein pharmaceuticals. Due to differences in diffusivity, large-scale freezing is not only associated with cryoconcentration (Hauptmann et al., 2019; Kolhe et al., 2012; Roessl et al., 2015), but can come with spatial shifts in the mAb to excipient ratio (Bluemel et al., 2020; Kolhe et al., 2012; Miller et al., 2013). In the present study, we connected freeze-concentration with frozen storage stability of mAbs. We examined

aggregation and oxidation of two mAbs formulated in histidine (mAb1) or adipic acid (mAb2). Samples were adjusted in the similar concentration range that evolves during cryoconcentration upon large-scale freezing (Bluemel et al., 2020). Two sets of samples were prepared for each mAb, one at a given mAb concentration and varying the buffer concentration and a second one with fixed buffer concentration but variation of the mAb concentration. Samples were stored at  $-10 \text{ }^\circ\text{C}$ , significantly above  $T_g'$ , to generate a stress model.

Formation of small soluble aggregates was analysed via SEC. Upon frozen storage, samples with varying mAb concentration showed only a marginal increase in HMWS levels of approximately 0.2%. Several studies emphasize a positive effect of protein concentration on stability (Arsiccio and Pisano, 2020; Jiang and Nail, 1998; Sarciaux et al., 1999). During freezing, mAbs adsorb at the ice/FCM interface. This interface area is finite and the relative adsorbed fraction decreases when mAb concentration is increased (Arsiccio and Pisano, 2020; Jiang and Nail, 1998). However, the sensitivity for denaturation and aggregation during freezing/thawing or freeze-drying is protein dependent (Jiang and Nail, 1998; Sarciaux et al., 1999). Furthermore, these studies focussed on the process conditions, whereas the recent study examines the storage stability of mAbs. While the mAb concentration did not affect HMWS levels upon frozen storage, an increase in histidine concentration increased the HMWS level by up to 4.8%. Protein-protein interactions highly depend on ionic strength (Wang et al., 2010) and can be correlated to the protein interaction parameter  $k_D$ . Positive  $k_D$  values are associated with net repulsive interactions (Menzen and Friess, 2014; Pindrus et al., 2018; Sorret et al., 2016). We found less repulsive interactions with higher buffer concentration, which can increase aggregation tendency in solution but also at the interface, where the adsorbed layer reflects a phase



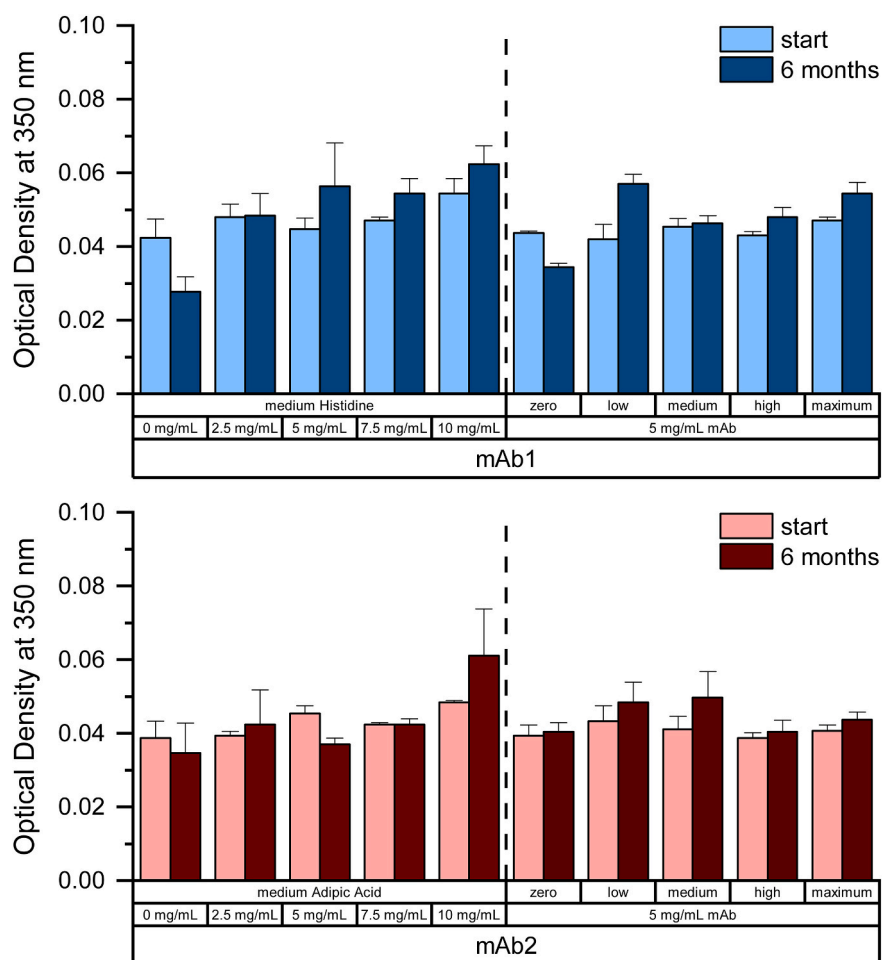


Fig. 3. OD<sub>350</sub> at the start and after six-month storage at  $-10^{\circ}\text{C}$ .

of high protein concentration with molecules fixed in close vicinity. Soluble aggregates in buffer-free samples increased by 5.6% and 5.8% upon six-month frozen storage of mAb1 and mAb2, respectively. This may be due to the pH of these samples that was not adjusted and differed from the histidine or adipic acid buffered solutions. This pH difference might also explain the higher HMWS levels at  $t_0$ . Due to the nonlinearity of the data under buffer-free conditions,  $k_D$  values cannot be reliably assessed to evaluate protein-protein interactions at the given pH and ionic strength (Pindrus et al., 2018; Sorret et al., 2016).

Larger aggregates were analysed via OD350 (Barnard et al., 2011; Jameel and Hershenson, 2010; Miller et al., 2013). No clear trends upon storage could be identified and no effects of mAb or buffer concentration. The negative impact of higher histidine concentrations on mAb1 stability, which was seen in SEC, was not reflected on this nanometre-size level, but was additionally pronounced at the micrometre level (see discussion on SVPs below). An influence of adipic acid concentration on mAb2 stability could not be detected via OD350. It has been shown previously that an increase in HMWS is not necessarily connected to an increase in turbidity (Singh et al., 2011).

Particles in the micrometre range were evaluated via flow imaging microscopy. Increasing mAb concentration led to higher SVPs counts up to approximately 100000 SVPs for mAb1 and 170000 SVPs for mAb2 upon six-month frozen storage. SVP formation steadily increased with mAb concentration for both mAbs, already seen at  $t_0$ , which included freeze-thaw stress. The significant increase in SVPs with mAb concentration presumably resulted from hundredth of a percent of the total protein in solution and is therefore not reflected in the HMWS levels (30). Increasing the buffer concentration and consequently the ionic

strength resulted in more pronounced formation of SVPs. Highest counts were detected for the maximum histidine (for mAb1 formulations) and maximum adipic acid concentration (for mAb2 formulations) with approximately 170000 SVPs and 100000 SVPs, respectively. During storage, protein-protein interactions contribute substantially to the overall stability, while especially surface-induced denaturation drives aggregation during the freezing and the thawing process (Duarte et al., 2020; Sarciaux et al., 1999; Singh et al., 2009). The decrease in  $k_D$  values with increasing histidine concentration showed a trend towards more attractive protein-protein interactions that was similarly observed for higher adipic acid concentration. While in buffer-free samples highest levels of soluble aggregates were detected, OD350 and SVPs remained on the initial level. Repulsive interactions between mAb aggregates presumably prevented the formation of large particles. Additionally performed dynamic light scattering measurements of buffer-free samples proved the general absence of particles in the micrometre range.

To our knowledge, no study examined the possible oxidation during frozen storage of proteins or mAbs. Authelin et al. emphasized the possible importance of mAb oxidation upon freezing (Authelin et al., 2020). Samples at lower temperatures per se contain high concentrations of oxygen due to an increase in oxygen solubility with decreasing temperature. In addition, dissolved gases freeze-concentrate as other solutes. As soon as the solubility limit is reached, gases, predominantly oxygen and nitrogen, can form air bubbles. This process is facilitated by cryoconcentration of other solutes, such as sugars or salts, which further reduce the solubility of gases. The practical relevance of freeze-concentration of oxygen has been shown by Takenaka et al. (Takenaka et al., 1996). In our study, we saw marked mAb oxidation as well as a

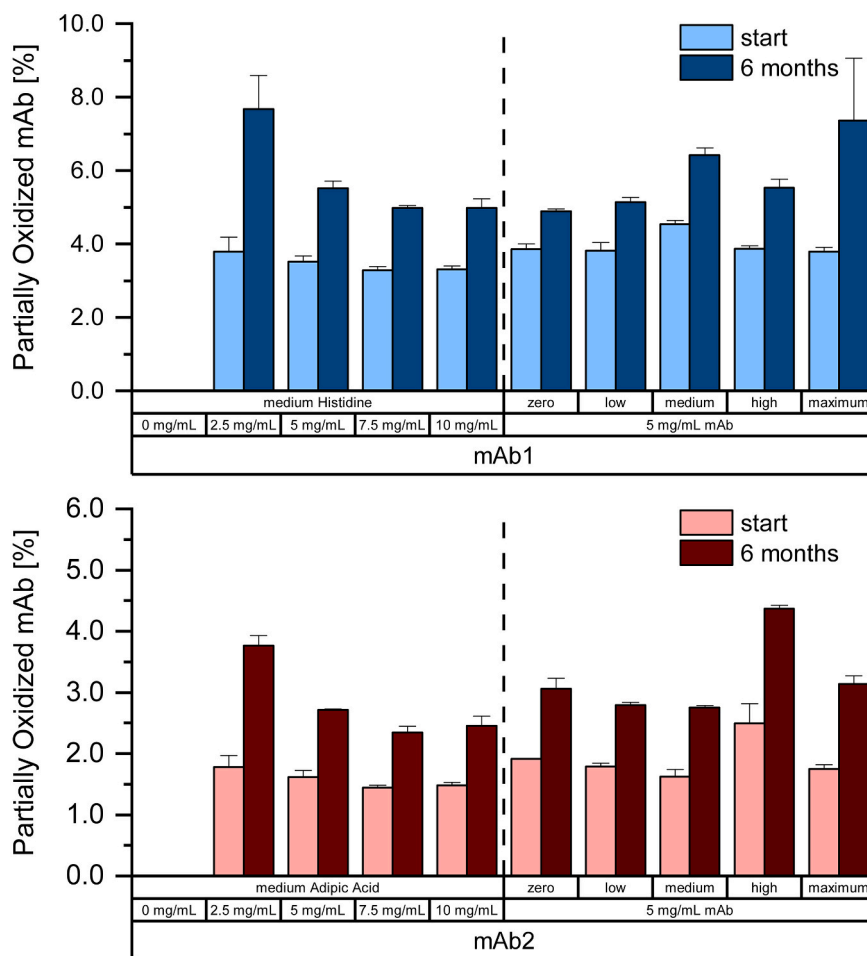


Fig. 4. mAb oxidation levels at the start and after six-month storage at  $-10\text{ }^{\circ}\text{C}$ .

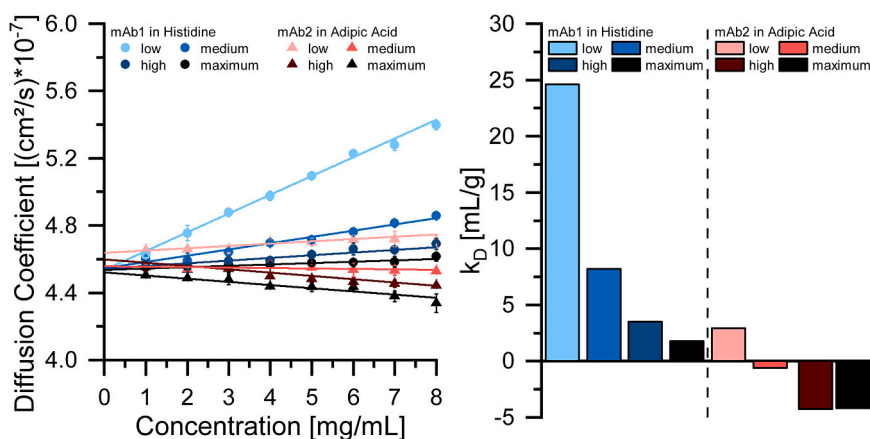


Fig. 5. Linear regression fit of diffusion coefficient versus protein concentration (left) and calculated  $k_D$  (right).

significant impact of mAb concentration on oxidation. In particular, at the lowest concentration of 2.5 mg/mL mAb1 or mAb2 the oxidation level after storage was substantially increased, whereas the different samples with a protein concentration between 5 mg/mL and 10 mg/mL showed a rather similar increase. At this point we could only speculate on rate limiting effects setting in at high protein concentration or enhancing effects at low protein concentration. No clear trend was observed for increasing adipic acid concentration, whereas higher histidine concentrations promoted mAb1 oxidation. Mason et al. have

demonstrated that histidine oxidises, accompanied by multiple byproducts, and that even pure histidine contains catalytic amounts of metal cations (Mason et al., 2010). The rapid oxidation of polysorbate 80 has been connected to the use of histidine buffer (Gopalrathnam et al., 2018); addition of a mAb completely prevented surfactant oxidation with the mAb potentially acting like a scavenger, which itself might get oxidised. Our experiment highlighted the need for a routine check of mAb oxidation during long-term frozen storage.

Transferred to cryoconcentration that we found upon large-scale

freezing in a 2 L bottle (Bluemel et al., 2020), our small-scale experiments suggest a marked impact of little changes in mAb and buffer concentration on mAb aggregation and oxidation. Depending on the position in the bottle, the stability significantly differs in comparison to the solution's initial nominal composition. Areas with the highest mAb concentration, found in the top region of the bottle, significantly contribute to the formation of SVPs. However, mAb oxidation is reduced in these regions. Due to differences in diffusivity, the mAb to buffer ratio is shifted towards the buffer component in the centre region near the bottom (Bluemel et al., 2020). This region can be associated with substantial formation of SVPs and, in case of the mAb1 formulation containing histidine, with higher HMWS levels and an increased partially oxidised mAb fraction. In contrast, the areas near the wall of the bottle, containing minimum buffer concentration, are characterised by highest stability. Overall, cryoconcentration should be avoided. One option is faster freezing, which could in addition reduce the exposure time of proteins to detrimental factors but may render smaller ice crystals and thus larger critical ice/FCM interface (Miller et al., 2013; Rodrigues et al., 2011). Alternatively, natural convection, which is thought to be the main driving force for freeze-concentration, could be reduced e.g. by freezing from bottom to top if the liquid level is low (Rodrigues et al., 2013). However, this would inevitably imply a new bottle and freezer design. Freezing solutions with lower mAb concentration may help to reduce SVP formation, but at the same time may increase the risk of mAb oxidation. The buffer concentration should be sufficient to stabilise the pH, but unnecessarily high concentrations coming with reduced repulsive mAb self-interaction should be avoided.

## 5. Conclusion

In this work, we examined the effects that changes in mAb and buffer concentration due to cryoconcentration have on long-term frozen storage stability. Two set of samples were prepared, one with constant mAb concentration (5 mg/mL mAb1 and mAb2, respectively) and a second one with constant buffer concentration (medium histidine/adipic acid). Concentrations were adjusted similarly to the position-dependent cryoconcentration that was found after large-scale freezing in a 2 L bottle (Bluemel et al., 2020). All samples were processed equally and subsequently stored for 6 months at  $-10^{\circ}\text{C}$ , significantly above  $T_g'$ .

Increasing mAb concentration did not affect the formation of HMWS upon long-term frozen storage, while higher histidine concentration facilitated the formation of HMWS. No effects of mAb or buffer species and concentrations on larger aggregates assessed via OD350 could be identified. The SVP count steadily increased for both mAbs with protein as well as buffer concentration. The protein-protein interaction parameter  $k_D$  revealed a trend towards more attractive interactions with higher ionic strength, i.e. buffer concentration. MAb oxidation upon frozen storage was found to be an important parameter, which was negatively affected by increasing histidine concentration, but became less with increasing mAb concentration. Transferred to spatial cryoconcentration in a large-scale 2 L bottle upon freezing (Bluemel et al., 2020), apparently small position-dependent changes in mAb and buffer concentration have a substantial impact on storage stability. Areas with higher mAb concentration, found in the top region, are prone to form SVPs, but show reduced levels of oxidised species. Regions with increased buffer concentration, in case of a 2 L bottle in the centre near the bottom, are associated with marked SVP levels. In case of mAb1 formulated in histidine, these areas additionally tend to form HMWS and oxidised mAb species. The highest stability is expected in regions near the wall that represent lowest buffer concentrations.

These finding suggest that reducing cryoconcentration, e.g. by accelerating freezing or directed freezing from bottom to top, can improve the long-term frozen storage stability of mAb solutions. Additionally, reducing the initial mAb concentration may help to decrease the formation of SVPs. However, this might increase the risk mAb oxidation. High buffer concentrations that reduce repulsive protein-

protein interactions should be avoided, but sufficiently high concentration assured to stabilise the formulation pH.

## Declaration of Competing Interest

The authors declare that they have no known competing financial interests or personal relationships that could have appeared to influence the work reported in this paper.

## Acknowledgements

The authors thank the Novartis Pharma AG for providing mAb stock solutions and Leonie Kainz for a helping hand during the sample preparation.

## References

- Arsiccio, A., Pisano, R., 2020. The ice-water interface and protein stability: a review. *J. Pharm. Sci.* 109, 2116–2130. <https://doi.org/10.1016/j.xphs.2020.03.022>.
- Arsiccio, A., McCarty, J., Pisano, R., Shea, J.-E., 2020. Heightened cold-denaturation of proteins at the ice–water interface. *J. Am. Chem. Soc.* 142, 5722–5730. <https://doi.org/10.1021/jacs.9b13454>.
- Authelin, J.-R., Rodrigues, M.A., Tchessalov, S., Singh, S.K., McCoy, T., Wang, S., Shalaev, E., 2020. Freezing of biologicals revisited: scale, stability, excipients, and degradation stresses. *J. Pharm. Sci.* 109, 44–61. <https://doi.org/10.1016/j.xphs.2019.10.062>.
- Barnard, J.G., Singh, S., Randolph, T.W., Carpenter, J.F., 2011. Subvisible particle counting provides a sensitive method of detecting and quantifying aggregation of monoclonal antibody caused by freeze-thawing: insights into the roles of particles in the protein aggregation pathway. *J. Pharm. Sci.* 100, 492–503. <https://doi.org/10.1002/jps.22305>.
- Bluemel, O., Buecheler, J.W., Rodrigues, M.A., Gerales, V., Hoelzl, G., Bechtold-Peters, K., Friess, W., 2020. Cryoconcentration and 3D temperature profiles during freezing of mAb solutions in large-scale PET bottles and a novel scale-down device. *Pharm. Res.* 37, 179. <https://doi.org/10.1007/s11095-020-02886-w>.
- Connolly, B.D., Le, L., Patapoff, T.W., Cromwell, M.E.M., Moore, J.M.R., Lam, P., 2015. Protein aggregation in frozen trehalose formulations: effects of composition, cooling rate, and storage temperature. *J. Pharm. Sci.* 104, 4170–4184. <https://doi.org/10.1002/jps.24646>.
- Duarte, A., Rego, P., Ferreira, A., Dias, P., Gerales, V., Rodrigues, M.A., 2020. Interfacial stress and container failure during freezing of bulk protein solutions can be prevented by local heating. *AAPS PharmSciTech* 21, 251. <https://doi.org/10.1208/s12249-020-01794-x>.
- Gervasi, V., Dall Agnol, R., Cullen, S., McCoy, T., Vucen, S., Crean, A., 2018. Parenteral protein formulations: an overview of approved products within the European Union. *Eur. J. Pharm. Biopharm.* 131, 8–24. <https://doi.org/10.1016/j.ejpb.2018.07.011>.
- Gopalrathnam, G., Sharma, A.N., Dodd, S.W., Huang, L., 2018. Impact of stainless steel exposure on the oxidation of polysorbate 80 in histidine placebo and active monoclonal antibody formulation. *PDA J. Pharm. Sci. Technol.* 72, 163–175. <https://doi.org/10.5731/pdajpst.2017.008284>.
- Hauptmann, A., Podgoršek, K., Kuzman, D., Srčić, S., Hoelzl, G., Loerting, T., 2018. Impact of buffer, protein concentration and sucrose addition on the aggregation and particle formation during freezing and thawing. *Pharm. Res.* 35, 101. <https://doi.org/10.1007/s11095-018-2378-5>.
- Hauptmann, A., Hoelzl, G., Loerting, T., 2019. Distribution of protein content and number of aggregates in monoclonal antibody formulation after large-scale freezing. *AAPS PharmSciTech* 20, 72. <https://doi.org/10.1208/s12249-018-1281-z>.
- Jameel, F., Hershenson, S., 2010. Formulation and process development strategies for manufacturing biopharmaceuticals. In: *Formulation and Process Development Strategies for Manufacturing Biopharmaceuticals*. John Wiley & Sons, Inc, Hoboken, NJ, USA. <https://doi.org/10.1002/9780470595886>.
- Jiang, S., Nail, S.L., 1998. Effect of process conditions on recovery of protein activity after freezing and freeze-drying. *Eur. J. Pharm. Biopharm.* 45, 249–257. [https://doi.org/10.1016/S0939-6411\(98\)00007-1](https://doi.org/10.1016/S0939-6411(98)00007-1).
- Kolhe, P., Amend, E., Singh, K., 2009. Impact of freezing on pH of buffered solutions and consequences for monoclonal antibody aggregation. *Biotechnol. Prog.* 26, 727–733. <https://doi.org/10.1002/btpr.377>.
- Kolhe, P., Mehta, A.P., Lary, A.L., Chico, S.C., Singh, S.K., 2012. Large-Scale Freezing of Biologicals (Part III). *BioPharm Int.* 25, 40–48.
- Kuelzto, L.A., Wang, W.E.L., Randolph, T.W., Carpenter, J.F., 2008. Effects of solution conditions, processing parameters, and container materials on aggregation of a monoclonal antibody during freeze-thawing. *J. Pharm. Sci.* 97, 1801–1812. <https://doi.org/10.1002/jps.21110>.
- Loew, C., Knoblich, C., Fichtl, J., Alt, N., Diepold, K., Bulau, P., Goldbach, P., Adler, M., Mahler, H.-C., Grauschopf, U., 2012. Analytical protein A chromatography as a quantitative tool for the screening of methionine oxidation in monoclonal antibodies. *J. Pharm. Sci.* 101, 4248–4257. <https://doi.org/10.1002/jps.23286>.
- Maity, H., Karkaria, C., Davagnino, J., 2009. Mapping of solution components, pH changes, protein stability and the elimination of protein precipitation during freeze–thawing of fibroblast growth factor 20. *Int. J. Pharmaceut.* 378, 122–135. <https://doi.org/10.1016/j.ijpharm.2009.05.063>.



- Mason, B.D., McCracken, M., Bures, E.J., Kerwin, B.A., 2010. Oxidation of Free L-histidine by tert-Butylhydroperoxide. *Pharm. Res.* 27, 447–456. <https://doi.org/10.1007/s11095-009-0032-y>.
- Menzen, T., Friess, W., 2014. Temperature-ramped studies on the aggregation, unfolding, and interaction of a therapeutic monoclonal antibody. *J. Pharm. Sci.* 103, 445–455. <https://doi.org/10.1002/jps.23827>.
- Miller, M.A., Rodrigues, M.A., Glass, M.A., Singh, S.K., Johnston, K.P., Maynard, J.A., 2013. Frozen-state storage stability of a monoclonal antibody: aggregation is impacted by freezing rate and solute distribution. *J. Pharm. Sci.* 102, 1194–1208. <https://doi.org/10.1002/jps.23473>.
- Padala, C., Jameel, F., Rathore, N., Gupta, K., Sethuraman, A., 2010. Impact of uncontrolled vs controlled rate freeze-thaw technologies on process performance and product quality. *PDA J. Pharm. Sci. Technol.* 64, 290–298.
- Pansare, S.K., Patel, S.M., 2016. Practical considerations for determination of glass transition temperature of a maximally freeze concentrated solution. *AAPS PharmSciTech* 17, 805–819. <https://doi.org/10.1208/s12249-016-0551-x>.
- Pikal-Cleland, K.A., Rodríguez-Hornedo, N., Amidon, G.L., Carpenter, J.F., 2000. Protein denaturation during freezing and thawing in phosphate buffer systems: monomeric and tetrameric  $\beta$ -galactosidase. *Arch. Biochem. Biophys.* 384, 398–406. <https://doi.org/10.1006/abbi.2000.2088>.
- Pindrus, M.A., Shire, S.J., Yadav, S., Kalonia, D.S., 2018. The effect of low ionic strength on diffusion and viscosity of monoclonal antibodies. *Mol. Pharm.* 15, 3133–3142. <https://doi.org/10.1021/acs.molpharmaceut.8b00210>.
- Rodrigues, M.A., Miller, M.A., Glass, M.A., Singh, S.K., Johnston, K.P., 2011. Effect of freezing rate and dendritic ice formation on concentration profiles of proteins frozen in cylindrical vessels. *J. Pharm. Sci.* 100, 1316–1329. <https://doi.org/10.1002/jps.22383>.
- Rodrigues, M.A., Balzan, G., Rosa, M., Gomes, D., de Azevedo, E.G., Singh, S.K., Matos, H.A., Geraldes, V., 2013. The importance of heat flow direction for reproducible and homogeneous freezing of bulk protein solutions. *Biotechnol. Prog.* 29, 1212–1221. <https://doi.org/10.1002/btpr.1771>.
- Roessler, U., Leitgeb, S., Nidetzky, B., 2015. Protein freeze concentration and micro-segregation analysed in a temperature-controlled freeze container. *Biotechnol. Rep.* 6, 108–111. <https://doi.org/10.1016/j.btre.2015.03.004>.
- Sarciaux, J.-M., Mansour, S., Hageman, M.J., Nail, S.L., 1999. Effects of buffer composition and processing conditions on aggregation of bovine IgG during freeze-drying. *J. Pharm. Sci.* 88, 1354–1361. <https://doi.org/10.1021/js980383n>.
- Singh, S.K., Kolhe, P., Wang, W., Nema, S., 2009. Large-scale freezing of biologics a practitioner's review, part one: fundamental aspects. *Bioprocess Int.* 7, 32–44.
- Singh, S.K., Kolhe, P., Mehta, A.P., Chico, S.C., Lary, A.L., Huang, M., 2011. Frozen state storage instability of a monoclonal antibody: aggregation as a consequence of trehalose crystallization and protein unfolding. *Pharm. Res.* 28, 873–885. <https://doi.org/10.1007/s11095-010-0343-z>.
- Sorret, L.L., DeWinter, M.A., Schwartz, D.K., Randolph, T.W., 2016. Challenges in predicting protein-protein interactions from measurements of molecular diffusivity. *Biophys. J.* 111, 1831–1842. <https://doi.org/10.1016/j.bpj.2016.09.018>.
- Takenaka, N., Ueda, A., Daimon, T., Bandow, H., Dohmaru, T., Maeda, Y., 1996. Acceleration mechanism of chemical reaction by freezing: the reaction of nitrous acid with dissolved oxygen. *J. Phys. Chem.* 100, 13874–13884. <https://doi.org/10.1021/jp9525806>.
- Wang, W., Nema, S., Teagarden, D., 2010. Protein aggregation—Pathways and influencing factors. *Int. J. Pharmaceut.* 390, 89–99. <https://doi.org/10.1016/j.ijpharm.2010.02.025>.
- Zhang, A., Singh, S.K., Shirts, M.R., Kumar, S., Fernandez, E.J., 2012. Distinct aggregation mechanisms of monoclonal antibody under thermal and freeze-thaw stresses revealed by hydrogen exchange. *Pharm. Res.* 29, 236–250. <https://doi.org/10.1007/s11095-011-0538-y>.